

Effect of spacing and skew-angle on clear-water scour at pier alignments

R. Lança

Instituto Superior de Engenharia, Universidade do Algarve, Faro, Portugal

C. Fael

Faculdade de Ciências da Engenharia, Universidade da Beira Interior, Covilhã, Portugal

R. Maia & J. Pêgo

Faculdade de Engenharia, Universidade do Porto, Porto, Portugal

A. H. Cardoso

Instituto Superior Técnico, Universidade Técnica de Lisboa, Lisboa, Portugal

ABSTRACT: Pier alignments, defined as single-row pier groups, displayed normal to main bridges' axes, are frequently used to support bridge decks. Different alignments configurations, characterized by different combinations of piers' shape and spacing and skew-angle of the alignment to the flow direction, lead to different interactions with the flow field and to different scour depths.

Twenty six long lasting – 7 to 15 days – laboratory experiments were run under steady clear-water flow conditions, close to the threshold condition of beginning of sediment motion, to address the effect of pier spacing and skew-angle on the equilibrium scour depth. Alignments consisted of four cylindrical piers spaced of 1, 2, 3, 4.5 and 6 pier diameters; tested skew-angles were 0°, 15°, 30°, 45° and 90°.

The main contribution of the paper derives from the long duration of the experiments. The functional relation of issued equilibrium scour depth with pier spacing and skew-angle is established and the dependence of the traditional group correction factor on the same variables is defined.

1 INTRODUCTION

Bridge decks are often supported by single-row pier groups, termed here as pier alignments. It is well known that piers located at alluvial river beds may induce the development of scour holes that, in extreme conditions, lead to structural bridge failures. The prediction of equilibrium scour depth is a key issue of bridge design, and this may be more difficult at pier alignments than at single piers due to the interaction of vortices and the concomitant interdependence of scour holes.

Many studies on local scouring at single piers have been carried out since the nineteen fifties; the corresponding results are widely published in the literature, including some engineering manuals (e.g. Breusers & Raudkivi (1991), Melville & Coleman (2000), Richardson & Davis (2001) or Sheppard & Renna (2010)).

Scouring at pier alignments requires and deserves additional research work since, by comparison with local scour studies at single cylindrical piers, few studies are reported in the literature. Those few that exist, authored by Hannah (1978), Elliot & Baker (1985), Salim & Jones (1996), Zhao & Sheppard (1998), Sumer & Fredsøe (2002), Ataie-Ashtiani & Beheshti (2006)), were indeed made in the context of,

mostly, short-duration scour studies at pile groups of complex piers. Since the methods available for the prediction of scour depth at complex piers – supposedly valid for pier alignments too – are based on a relatively small number of short-duration experiments, the obtained results inherently carry a considerable degree of uncertainty.

This study is focused in further characterizing the effect of pier spacing and alignment skew-angle on the maximum clear-water scour depth at pier alignments consisting of four cylindrical piers. The accuracy of two methods used in engineering practice to predict scour depth at pier alignments is also assessed.

2 FRAMEWORK FOR ANALYSIS

According to Fael (2007), clear-water scour at single cylindrical piers inserted in wide rectangular channels, whose bed is composed of uniform non-ripple forming sand, can be demonstrated to be dependent on the following set of non-dimensional parameters, Fael (2007),

$$\frac{d_s}{D_p} = \Phi \left(\frac{d}{D_p}; \frac{U}{U_c}; \frac{D_p}{D_{50}}; \frac{Ut}{D_p} \right) \quad (1)$$

as soon as the approach flow is fully developed and uniform and the flow inside the scour hole is rough turbulent (free of viscous effects). In Equation 1, d_s = scour depth; D_p = pier diameter; d = approach flow depth; U = approach flow velocity; U_c = approach flow velocity for the threshold condition of sediment entrainment; D_{50} = median sediment size; t = time; d/D_p = flow shallowness or relative approach flow depth; U/U_c = flow intensity; D_p/D_{50} = sediment coarseness or relative sediment size; Ut/D_p = non-dimensional time.

It should be noted here that i) by fully developed flow, it is meant that the boundary layer covers the entire flow depth; ii) it is assumed that wall effects are negligible and the velocity field is bi-dimensional at the central zone of the channel where the pier alignment is placed as soon as $B/d > 5$, B = channel width; iii) sand is considered uniform if $\sigma_D < 1.5$ (σ_D = sediment gradation coefficient); iv) and ripples do not occur if $D_{50} > 0.6$ mm.

Assuming the definition of additional variables included in Figure 1, Equation 1 can be generalized for pier alignments as

$$\frac{d_s}{D_p} = \varphi \left(\frac{d}{D_p}; \frac{U}{U_c}; \frac{D_p}{D_{50}}; \frac{Ut}{D_p}; \frac{s}{D_p}; \alpha; K_f; m \right) \quad (2)$$

where s = pier spacing; α = alignment skew-angle; K_f = pier shape coefficient; m = number of piers in the alignment.

It is worth to note that n parallel alignments form pile groups commonly integrated in complex piers. In

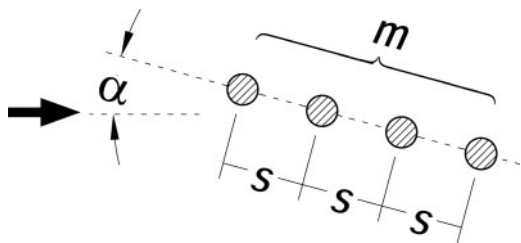


Figure 1. Characteristic variables of a pier alignment.

the case of piles groups supporting un-submerged pile caps, Equation 2 can still be generalized as follows:

$$\frac{d_s}{D_p} = \varphi \left(\frac{d}{D_p}; \frac{U}{U_c}; \frac{D_p}{D_{50}}; \frac{Ut}{D_p}; \frac{s}{D_p}; \alpha; K_f; m; n \right) \quad (3)$$

For i) $d/D_p \geq \sim 4$, where scour depth is maximized and does no longer depend much on the approach flow depth; ii) cylindrical piers ($K_f = 1$) and iii) at the equilibrium stage, characterized by the fact that d_s is independent from t (denoted as d_{se}), Equation 3 is written as:

$$\frac{d_{se}}{D_p} = \varphi \left(\frac{U}{U_c}; \frac{D_p}{D_{50}}; \frac{s}{D_p}; \alpha; m; n \right) \quad (4)$$

For $U/U_c = 1$, where d_{se} is known to be maximal, and assuming D_p/D_{50} to be restricted to a narrow range of values, Equation 4 becomes:

$$\frac{d_{se}}{D_p} = \varphi \left(\frac{s}{D_p}; \alpha; m; n \right) \quad (5)$$

The parameters of Equations 4 and 5 constitute the framework of analysis of the studies previously mentioned in the Introduction (see Table 1).

From Table 1, it is clear that the typical duration, t_d , of the experiments reported in the literature is rather short as compared to the time needed to approach the equilibrium phase. Yet, it should be noted here that some of the authors have made one or two longer validation experiments. According to Simarro *et al.* (2011), the duration of the experiments should be, at least, 7 days, to allow for the adequate prediction of equilibrium scour at single cylindrical piers. This minimum duration is possibly optimistic for pier alignments since the scouring process can be anticipated to be more complex and slower. Consequently, conclusions issued from the mentioned studies do not seem to guarantee accurate predictions of the equilibrium scour depth at pile groups and pier alignments.

In the studies characterized in Table 1, the sand was always uniform; with the exception Hannah (1978),

Table 1. Control variables and non-dimensional parameters of studies known to date.

| Author | $\alpha(^{\circ})$ | s/D_p | n | m | U/U_c | t_d (h) | Shape ⁽¹⁾ |
|------------------|--------------------|----------|---------|---------|---------|-------------|----------------------|
| H | 0–90 | 1–21 | 1 | 2 | 0.7 | ≈ 7 | Circular |
| E&B | 0 | 1.6–13.2 | 1 | 3 | 0.5–1.0 | NS | RC |
| S&J | 0–50 | 1–10 | 3 | 3 | 1.0 | 4 | Square |
| Z&S | 0–90 | 3 | 3 | 8 | 0.65 | 26 | C+S |
| A&B | 0 | 1–11 | 1; 2; 3 | 1; 2; 3 | 0.7–0.9 | ≈ 8 | Circular |
| A ⁽²⁾ | 0 | 1–6 | 2; 3 | 2; 4; 5 | 0.95 | ≈ 8 | Circular |

H = Hannah (1978); E&B = Elliot & Baker (1985); S&J = Salim & Jones (1996); Z&S = Zhao & Sheppard (1999); A&B = Ataie-Ashtiani & Beheshti (2006); A = Amini *et al.* (2012); C+S = circular and square; RC = round nose rectangular; NS = non-specified.

⁽¹⁾ shape of the pier cross-section; ⁽²⁾ experiments on uniform spacing and un-submerged pile groups.

Amini *et al.* (2012) and, in some cases, Ataie-Ashtiani & Beheshti (2006), the remaining authors have used fine sand, prone to lead to the formation of ripples in the approach flow reach. In the study of Salim & Jones (1996), ripples have certainly shown up since $U/U_c \approx 1.0$.

In general, the quoted authors concluded that the maximum scour depth decreases with the increase of the spacing between the piles. Exceptionally, Ataie-Ashtiani & Beheshti (2006) reported that for two piles aligned with the approach flow, i.e., $\alpha = 0^\circ$, the maximum scour depth is observed for $s/D_p = 3$; the same authors also report that, for $\alpha = 90^\circ$, the maximum scour depth occurs for $s/D_p = 1$.

For the scour depth prediction at pile groups defined by $\alpha = 0^\circ$, Salim & Jones (1996) – who worked on square cross-section piles – suggested that the scour depth is equal to the one obtained at a rectangular pier whose dimensions are equal to the sum of the individual piles sides. These authors also concluded that i) the effect of the skew-angle on the scour depth at the pile group and at the equivalent solid pier can be considered the same and ii) the skew-angle that maximizes scour depth is $\alpha = 30^\circ$. According to Zhao & Sheppard (1999), the maximum scour depth is observed for $\alpha = 25^\circ$ in the case of pile groups made of cylindrical piles.

Amini *et al.* (2012) – who focused their study on pile groups with $\alpha = 0^\circ$ – suggested that, for $s/D_p = 1$, the pile group produces one single horse-shoe vortex and the scour pattern is similar to the one produced by a single pier. For $s/D_p \leq 3.5$, the pile group still produces one single scour hole; when $s/D_p > 3.5$, the interference between adjacent piles diminishes and incipient individual scour holes can be observed. With further increases of s/D_p , the individual scour holes tend to separated and, for $s/D_p > 5$, each pile has one clearly individualized scour hole; consequently the maximum scour depth of the pile group becomes independent from s/D_p for $s/D_p > 5$.

Some of the predictors used in engineering practice to calculate the equilibrium scour depth at pile groups are based on methods initially developed for single cylindrical piers. In the cases of Richardson and Davis (2001) and Sheppard & Renna (2010), the concept of equivalent diameter emerges. The equivalent diameter is defined as the diameter of a single cylindrical pier that leads to the same equilibrium depth as the pile group. In the case of non-submerged cylindrical pile groups, the equivalent diameter depends on the non-overlapping individual pile widths, projected in a plane normal to the approach flow, L_{pg} , as well as on coefficients that account for i) the pile spacing, K_s , and ii) the number of rows aligned with the approach flow, K_m , if $\alpha < 5^\circ$.

The objective of this study is to contribute to the improved characterization of the equilibrium scour depth at pier alignments on the basis of systematic experimentation. The most important difference of this study as compared with those carried out in the past consists in the long duration of the experiments.

3 EXPERIMENTAL SETUP

Two flumes were used in the experimental study. One of them is 28.00 m long, 2.00 m wide and 1.00 m deep and it includes a closed hydraulic circuit whose maximum flow discharge is $0.135 \text{ m}^3 \text{ s}^{-1}$. Discharge is measured with an electromagnetic flow meter installed in the circuit. At the entrance of the flume, two honeycomb diffusers aligned with the flow direction smooth the flow trajectories and guarantee the lateral uniform flow distribution. Immediately downstream from the diffusers, a 5.00 m long bed reach is covered with fine gravel, to provide proper roughness and guarantee fully developed flow. The central reach of the flume, starting at 14.00 m from the entrance, includes a 3.00 m long, 2.00 m wide and 0.60 m deep recess box in the bed. At the downstream end of the flume, a tailgate allows for the regulation of the water depth. The water falls into a 100 m^3 reservoir, where the hydraulic circuit starts.

The bed recess box was filled with uniform quartz sand ($\rho_s = 2650 \text{ kgm}^{-3}$; $D_{50} = 0.86 \text{ mm}$; $\sigma_D = 1.36$).

The experiments were carried out with a constant approach flow depth, $d = 0.20 \text{ m}$, and average velocity, U , approximately equal to the critical velocity for sediment entrainment, $U_c \approx 0.33 \text{ ms}^{-1}$. For this velocity, the scour depth can be expected to be maximal as soon as the remaining parameters of Equation 3 are kept constant.

Individual cylindrical piers were simulated by PVC pipes with diameter $D_p = 50 \text{ mm}$. Alignments of four piers were placed approximately at the center of the bed recess box; both the pier spacing and the alignment skew-angle were systematically varied: $s/D_p = \{1, 2, 3, 4.5, 6\}$; $\alpha = \{0^\circ, 15^\circ, 30^\circ, 45^\circ, 90^\circ\}$. The choice of four piers per alignment was made assuming that a bigger number of piers would not impact the conclusions.

The second flume differs from the previously described one in its dimensions. It is 33.15 m long, 1.00 m wide and 1.0 m deep; its central reach starts at 16.00 m from the entrance; the maximum flow discharge is $0.090 \text{ m}^3 \text{ s}^{-1}$; the depth of the recess box is 0.35 m. The sand used in this flume as well as control variables such as flow depth and velocity, diameter of individual piers, m and spacing were the same as in the first flume. Due to width restrictions, it was used to run experiments with small skew-angles to avoid wall and contraction effects.

Prior to each experiment, the sand bed was leveled with the adjacent concrete bed. The area located around the pier alignment was covered with a thin metallic plate to avoid uncontrolled scour at the beginning of each experiment. Flumes were filled gradually through independent small-discharge hydraulic circuits, imposing high water depth and low flow velocity. The discharge corresponding to the chosen approach flow velocity was then passed through each flume. The flow depth was regulated by adjusting the downstream tailgates. Once the discharge and flow depth were established, the metallic plates were removed and the experiments started.

Scour immediately initiated and the depth of scour hole was measured at each individual pier, to the accuracy of ± 1 mm, with adapted point gauges, with a high frequency during the first day. Afterwards, the interval between measurements increased and three or four measurements were carried out per day. When the scour rate was less than ~ 2 mm ($\sim 2D_{50}$) in 24 hour and at least ~ 7 days had passed, the experiments were stopped. The sand bed approach reach located upstream the piers was verified to stay undisturbed along the entire duration of the experiments; this long term stability ensured that scour depth did not add with upstream bed degradation.

4 RESULTS AND DISCUSSION

Twenty six experiments were carried out. One of them was run for a single cylindrical pier ($D_p = 50$ mm). Table 2 records the main variables and non-dimensional parameters of the twenty five experiments run for pier alignments; it includes the alignment skew-angle, α , pier spacing, s , the normalized pier spacing, s/D_p , the sum of the non-overlapping individual pier widths projected on a plane normal to the approach flow, L_{pg} , and the experiment duration, t_d .

The flow shallowness, $d/D_p = 4.00$, flow intensity, $U/U_c \approx 1.00$, and sediment coarseness, $D_p/D_{50} \approx 60$, were chosen so as to maximize the alignment scour depth, d_{sepg} (Sheppard *et al.* (2004)). The ratio $B/d = \{5, 10\}$ guarantees the absence of wall effects. The ratio B/L_{pg} was typically bigger than 10 as a precaution to avoid contraction scour. In a few cases, for $\alpha = 15^\circ$, the ratio went down to 5, as the experiments on this skew-angle were made in the 1.0 m wide flume. In no case contraction scour was observed, since the borders of the scour holes never reached the walls of the flumes.

It is postulated here that equilibrium is attained asymptotically. Consequently, the time records of scour depth were extrapolated to $t = \infty$ through the 6-parameter polynomial technique suggested by Lança *et al.* (2010) as a means to estimate the equilibrium scour depth associated to each pier. The corresponding maxima, d_{sepg} , as well as their ratios to the reference equilibrium scour depth produced at the single cylindrical pier, d_{sepg}/d_{se1} , are also included in Table 2. The location of the deepest scour hole changed from experiment to experiment and d_{sepg} attends to this fact. The reference scour depth was $d_{se1} = 0.136$ m, leading to $d_{se1}/D_p = 2.72$. This value compares with $d_{se}/D_p = 2.4$, as suggested by authors such as Melville & Coleman (2000), and the increase is possibly ascribable to the long duration of the test as well as to the extrapolation of the scour records to infinite time.

It should be noticed that pier alignments defined by $s/D_p = 1$ can be assumed to behave as one equivalent single pier whose shape is that of a round-nose rectangular pier, as sketched in Figure 2 (dashed perimeter).

Table 2. Control variables of the experiments and equilibrium scour depths.

| Exp. | α ($^\circ$) | s (m) | s/D_p | L_{pg} (m) | t_d (day) | d_{sepg} (m) | d_{sepg}/d_{se1} |
|------|-----------------------|---------|---------|--------------|-------------|----------------|--------------------|
| 1 | 0 | 0.050 | 1.0 | 0.050 | 11.0 | 0.153 | 1.13 |
| 2 | | 0.100 | 2.0 | 0.050 | 16.0 | 0.160 | 1.18 |
| 3 | | 0.150 | 3.0 | 0.050 | 13.7 | 0.152 | 1.12 |
| 4 | | 0.225 | 4.5 | 0.050 | 16.2 | 0.184 | 1.36 |
| 5 | | 0.300 | 6.0 | 0.050 | 11.2 | 0.136 | 1.00 |
| 6 | 15 | 0.050 | 1.0 | 0.089 | 11.2 | 0.157 | 1.15 |
| 7 | | 0.100 | 2.0 | 0.128 | 13.2 | 0.152 | 1.12 |
| 8 | | 0.150 | 3.0 | 0.167 | 15.4 | 0.162 | 1.19 |
| 9 | | 0.225 | 4.5 | 0.200 | 8.9 | 0.183 | 1.35 |
| 10 | | 0.300 | 6.0 | 0.200 | 11.2 | 0.170 | 1.25 |
| 11 | 30 | 0.050 | 1.0 | 0.125 | 6.9 | 0.246 | 1.81 |
| 12 | | 0.100 | 2.0 | 0.200 | 6.9 | 0.242 | 1.78 |
| 13 | | 0.150 | 3.0 | 0.200 | 7.7 | 0.212 | 1.56 |
| 14 | | 0.225 | 4.5 | 0.200 | 7.2 | 0.198 | 1.46 |
| 15 | | 0.300 | 6.0 | 0.200 | 7.7 | 0.177 | 1.30 |
| 16 | 45 | 0.050 | 1.0 | 0.156 | 7.9 | 0.316 | 2.33 |
| 17 | | 0.100 | 2.0 | 0.200 | 6.9 | 0.174 | 1.28 |
| 18 | | 0.150 | 3.0 | 0.200 | 9.9 | 0.149 | 1.09 |
| 19 | | 0.225 | 4.5 | 0.200 | 8.2 | 0.158 | 1.16 |
| 20 | | 0.300 | 6.0 | 0.200 | 7.9 | 0.144 | 1.06 |
| 21 | 90 | 0.050 | 1.0 | 0.200 | 10.3 | 0.354 | 2.61 |
| 22 | | 0.100 | 2.0 | 0.200 | 9.6 | 0.190 | 1.40 |
| 23 | | 0.150 | 3.0 | 0.200 | 9.4 | 0.175 | 1.29 |
| 24 | | 0.225 | 4.5 | 0.200 | 7.2 | 0.159 | 1.17 |
| 25 | | 0.300 | 6.0 | 0.200 | 7.8 | 0.127 | 0.94 |

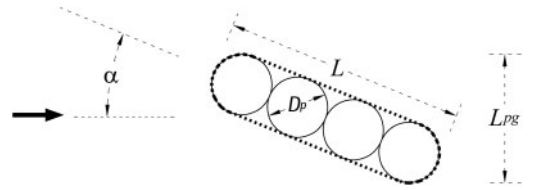


Figure 2. Equivalent single pier defined for $s/D_p = 1$.

The associated ratio of pier length to pier width is, in this study, $L/D_p = 4$.

Assuming that the above conceptualization is right, the following equation should hold:

$$d_{sepg}|_{\alpha} = K_{\alpha} K_f (d_{sepg}|_{\alpha=0}) \quad (6)$$

where K_{α} = skew-angle factor and K_f = pier shape factor, while the remaining symbols are self explanatory.

Figure 3 presents the time records of the scour depth at the pier alignments by exploiting two key control variables of the experiments, *i.e.*, the skew angle, α , and the normalized pier spacing, s/D_p . The longer records are truncated at $t = 200$ h and the scale of d_s is the same for all experiments. The reference equilibrium scour depth, d_{se1} , is also represented. The pier P1 is the pier located the most upstream and the pier P4 is the most downstream, with the exception of the experiments defined by $\alpha = 90^\circ$, where the concepts of upstream and downstream no longer apply.

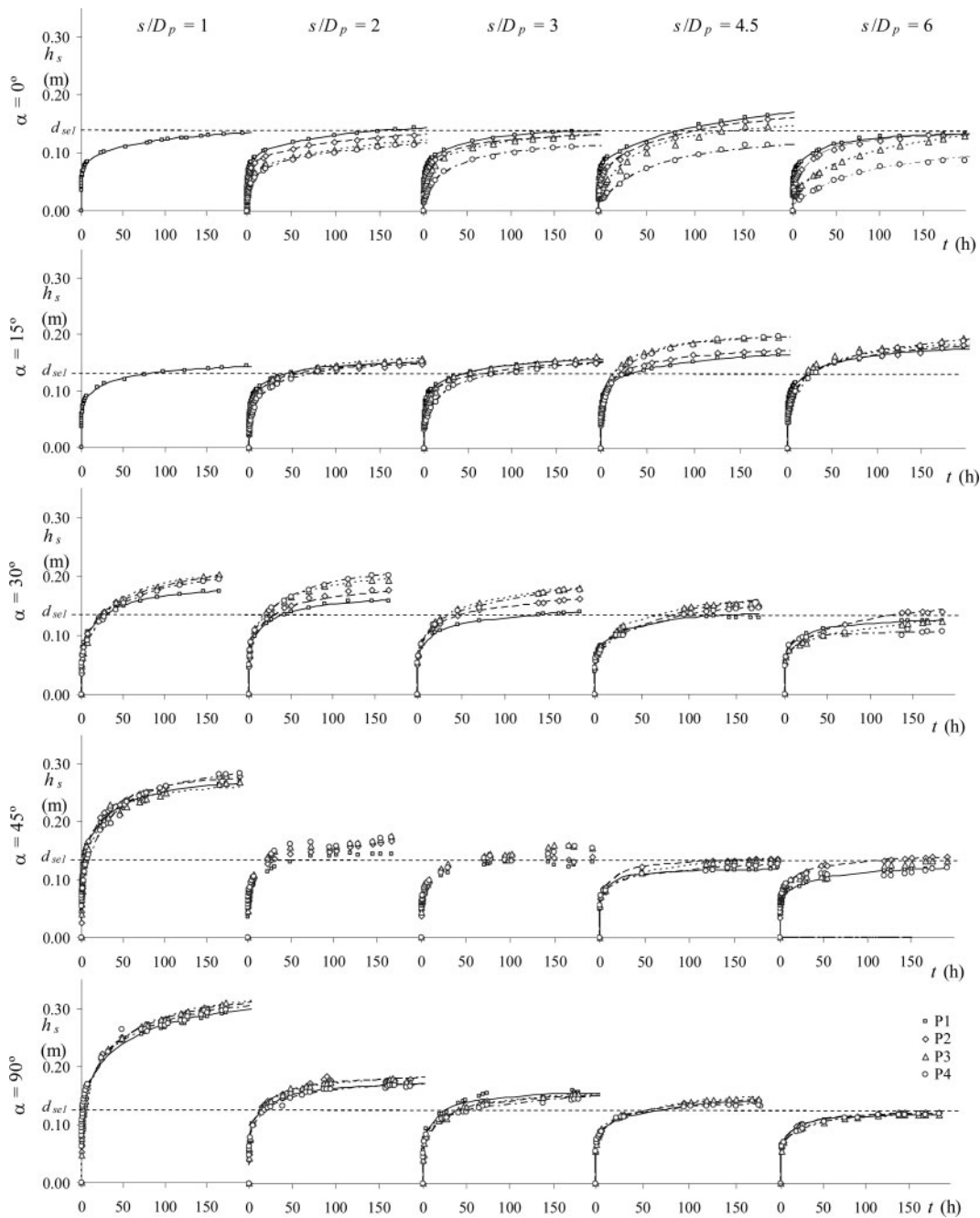


Figure 3. Scour depth time evolution at pier alignments for $\alpha = \{0^\circ; 15^\circ; 30^\circ; 45^\circ; 90^\circ\}$ and $s/D_p = \{1.0; 2.0; 3.0; 4.5; 6.0\}$.

From Figure 3 and Table 2, the following important conclusions can be drawn:

- i) For $\alpha = 0^\circ$, the deepest scour hole is always observed at the pier P1. The fact that scour holes are shallower at the remaining piers in the alignment is possibly induced by the effect of “shadow”, *i.e.*, to the decrease of the approach

flow velocity – since mass is diverted by the piers located upstream – as well as by the deposition of sand originated at upstream scours holes. The maximum scour depth, recorded at the pier P1, is approximately 15% higher than the reference scour depth, d_{sel} (see Table 2), for $s/D_p = \{1, 2, 3\}$; this increase more than doubles for $s/D_p = 4.5$ and vanishes for $s/D_p = 6$. For small values of

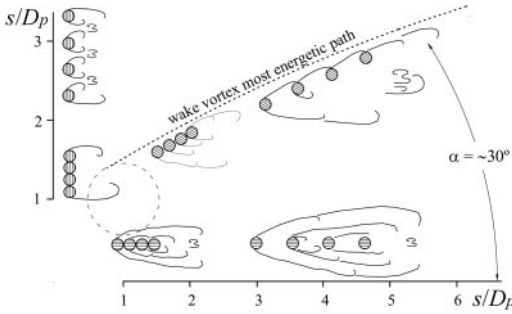


Figure 4. System of wake vortices at pier alignments.

s/D_p , the scour depth increase can be explained by the interaction of the horse-shoe vortices at individual piers; on top of that, the wake vortices originated at the sides of piers P2 to P4 provide extra siphoning strength and capacity to transport sand downstream, as compared with the situation observed at single cylindrical piers, this way contributing to increase the maximum scour depth at the pier group; the combination of these two effects seems to be maximal for $s/D_p = 4.5$ and then vanish for $s/D_p = 6$. This result is not much different from the suggestion of Ashtiani & Beheshti (2006) who reported the maximum scour depth for $s/D_p = 3$, as $\alpha = 0^\circ$.

- ii) When $\alpha = 15^\circ$, the scour depth time evolution is approximately the same at the four piers in the alignment, except for $s/D_p = 4.5$ where the deepest scour hole is observed at P4. On top of that, the values of d_{sepg}/d_{se1} are not significantly different from those observed for $\alpha = 0^\circ$, conflicting with intuition and some findings reported in the literature (e.g. Zhao & Sheppard (1999)).
- iii) For $\alpha = \{30^\circ; 45^\circ; 90^\circ\}$, scour depth systematically decreases with s/D_p .
- iv) For $s/D_p = 6$, scour depth shows a weak dependence on α . Yet, $\approx 25\%$ – 30% scour increase is observed for $\alpha = \{15^\circ; 30^\circ\}$, as compared with the isolated cylindrical pier.
- v) With the exception of $s/D_p = 1$, the deepest scour holes are observed for $\alpha = 30^\circ$ and $s/D_p = \{2; 3\}$. In these cases, piers downstream of P1 are located in the path of highly energetic wake vortices originated upstream (see Figure 4), and the maximum scour depth is observed at P3 or P4 for all s values except $s/D_p = 6$ (where it occurs at P2). The ratio d_{sepg}/d_{se1} is ≈ 1.7 and it slightly decreases until 1.3 for $s/D_p = 6$.
- vi) For $\alpha = 45^\circ$, small oscillations are observed in the scour depth time evolution, especially for $s/D_p = \{2; 3\}$ (see Figure 3). It can be speculated that these oscillations occur due to the interaction of horse-shoe vortices arms with wake vortices separated from the upstream pier. This explanation requires experimental confirmation. The ratio d_{sepg}/d_{se1} is ≈ 2.3 for $s/D_p = 1$ and clearly decreases with s/D_p ; $d_{sepg}/d_{se1} \approx 1.3$ when $s/D_p = 2$.

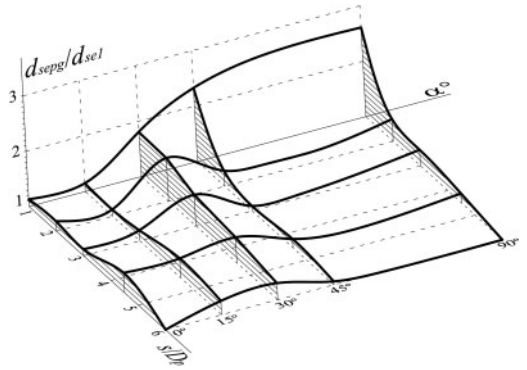


Figure 5. Variation of d_{sepg}/d_{se1} with s/D_p and α .

- vii) When $\alpha = 90^\circ$, the scour depth time evolution presents minor differences at different piers; it seems though that the thalweg is located at P2 or P3. For $s/D_p = 1$, the pier acts as a single pier with one single horse-shoe vortex. The scour depth is the biggest. For $s/D_p = 2$, different horse-shoe vortices are believed to be present, the corresponding arms being compressed by the flow acceleration in the spacing between piers. With the increase of s/D_p , this group effect tends to vanish and each pier in the alignment tends to behave as a single one. The ratio d_{sepg}/d_{se1} is ≈ 2.6 for $s/D_p = 1$, $d_{sepg}/d_{se1} \approx 1.35$ for $s/D_p = \{2; 3\}$ and $d_{sepg}/d_{se1} \approx 1$ for $s/D_p = 6$.

Most of the previous conclusions are translated in Figure 5 where the ratio d_{sepg}/d_{se1} is plotted against s/D_p and α .

Keeping in mind the pier conceptualization of Figure 2, it is possible to reproduce, within an error margin of 10%, the equilibrium scour depths measured for $s/D_p = 1$ by assuming $K_f = 1$ (valid for round-nose rectangular piers) and $K_\alpha = \{2.0; 2.3; 2.5\}$ for, respectively, $\alpha = \{30^\circ; 45^\circ; 90^\circ\}$, as suggested by Richardson & Davis (2001).

For the most common s/D_p values used in engineering practice, i.e., $s/D_p > \approx 3$, the equilibrium scour depth increases $\{15\%; 30\%; 30\%; 10\%; 10\%\}$ for, respectively, $\alpha = \{0^\circ; 15^\circ; 30^\circ; 45^\circ; 90^\circ\}$ as compared with the expected value at a single cylindrical pier with the same diameter, D_p , as the individual piers. This shows that, for $s/D_p > 3$, the worst skew-angles tend to be in the range of $15^\circ \leq \alpha \leq 30^\circ$.

The data set obtained in this study constitutes an independent basis for the assessment of existing predictors of scour depth at pile groups and pier alignments. For this reason, the predictions issued by the methods of Richardson & Davis (2001) and Sheppard & Renna (2010) were compared with measurements. Figure 6 displays the values of d_{sepg}/d_{se1} predicted by both methods against the corresponding measured values. Deviation bands of 25 and 40% towards perfect agreement are also included; d_{se1} stands, in both axes, for the measured value.

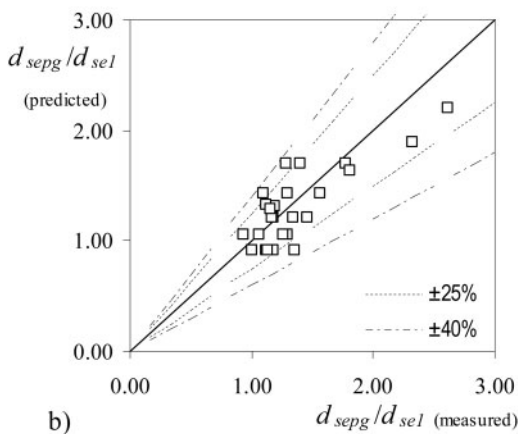
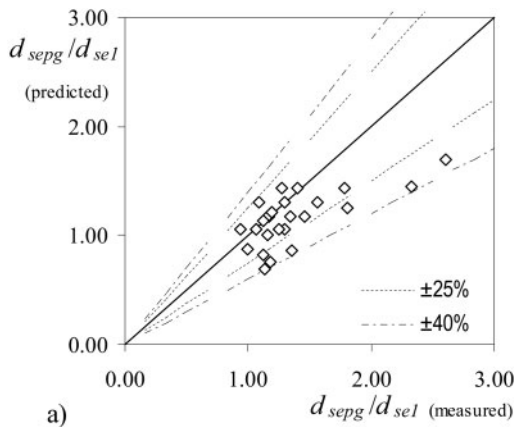


Figure 6. Measured d_{sepg}/d_{se1} v.s. corresponding predictions, according to a) Richardson & Davis (2001) and b) Sheppard & Renna (2010).

From the inspection of Figure 6, it can be concluded that an important number of measurements exceed the corresponding predictions. This is more evident for the method of Richardson & Davis (2001). It is also worth of notice that some measurements exceed the predictions by approximately 40%, which is rather significant.

5 CONCLUSIONS

From the previous discussion, the following summary of conclusions can be drawn:

- i) When $\alpha = \{0^\circ; 15^\circ\}$, $d_{sepg}/d_{se1} < 1.35$ and the maxima scour depths occur for $s/D_p \approx 4.5$.
- ii) For $\alpha = \{30^\circ; 45^\circ; 90^\circ\}$, the scour depth systematically decreases with s/D_p .
- iii) When $s/D_p = 6$, $d_{sepg}/d_{se1} \approx 1.25-1.30$ for $\alpha = \{15^\circ; 30^\circ\}$, while $d_{sepg}/d_{se1} \approx 1$ for the remaining skew-angles.
- iv) When $s/D_p = 1$, the pier alignment can be treated as a single round-nose rectangular pier whose

cross-section is defined as the envelope of the adjacent piers.

- v) Excluding $s/D_p = 1$ the maximum scour depth occurs for $\alpha = 30^\circ$ and $s/D_p = \{2; 3\}$, where $d_{sepg}/d_{se1} \approx 1.7$.
- vi) Common methods applied in engineering practice to predict scour depth at pier alignments may provide under-predictions of the order of up to 40%.

ACKNOWLEDGEMENTS

The authors wish to acknowledge the financial support of the Portuguese Foundation for Science and Technology through the research project PTDC/ECM/101353/2008.

REFERENCES

- Amini, A.; Melville, B.; Ali, T. M.; Ghazali, A. H. Clearwater local scour around pile groups in shallow-water flow. *Journal of Hydraulic Engineering*, in press.
- Ataie-Ashtiani, B.; Beheshti, A. A. 2006. Experimental investigation of clear-water local scour at pile groups. *Journal of Hydraulic Engineering*, 132(10): 1100–1104.
- Breusers, N. H. C.; Raudkivi, A. J. 1991. *Scouring*. Rotterdam (The Netherlands), Balkema.
- Elliot, K. R.; Baker, C. J. 1985. Effect of pier spacing on scour around bridge piers. *Journal of Hydraulic Engineering*, 111(7): 1105–1109.
- Fael, C.S. 2007. *Erosões localizadas junto de encontros de pontes e respectivas medidas de protecção*. Covilhã (Portugal): Universidade da Beira Interior.
- Hannah, C. R. 1978. *Scour at pile groups*. Canterbury (New Zealand): University of Canterbury.
- Lança, R.; Fael, C.; Cardoso, A. H. 2010. Assessing equilibrium clear-water scour around single cylindrical piers. *Proc. River Flow 2010*. Braunschweig (Germany), 8–10 September.
- Melville, B. W.; Coleman, S. E. 2000. *Bridge scour*. Colorado (U.S.): Highlands Ranch Water Resources.
- Richardson, E. V.; Davis, S. R. 2001. *Evaluating scour at bridges*. Forth Collins (U.S.): Federal Highway Administration.
- Salim, M.; Jones, J. S. 1996. Scour around exposed pile foundations. *Proc. of the American Society of Civil Engineers "North American Water and Environment Congress '96"*, Anaheim (U.S.).
- Sheppard, D. M.; Odeh, M.; Glasser, T. 2004. Large scale Clearwater local pier scour experiments. *Journal of Hydraulic Engineering*, 130(10): 957–963.
- Sheppard, D. M.; Renna, R. 2010. *Florida Scour Manual*. Florida (U.S.): Florida Department of Transportation.
- Simarro, G.; Fael, C.M.S.; Cardoso, A. H. 2011. Estimating equilibrium scour depth at cylindrical piers in experimental studies". *Journal of Hydraulic Engineering*, 137(9): 1089–1093.
- Sumer, B. M.; Fredsøe, J. 2002. *The Mechanics of Scour in the Marine Environment, Advanced Series on Ocean Engineering*. Singapore: World Scientific Publishing Co. Pte. Ltd.,
- Zhao, G.; Sheppard, D. M. 1999. The effect of flow skew angle on sediment scour near pile groups. *Stream Stability and Scour at Highway Bridges; Compilation of Conference Papers*, Reston (U.S.): ASCE.